Cell Reports Medicine, Volume *5*

Supplemental information

Targeting of vulnerabilities of drug-tolerant persisters identified through functional genetics delays tumor relapse

Mengnuo Chen, Sara Mainardi, Cor Lieftink, Arno Velds, Iris de Rink, Chen Yang, Hendrik J. Kuiken, Ben Morris, Finn Edwards, Fleur Jochems, Olaf van Tellingen, Manon Boeije, Natalie Proost, Robin A. Jansen, Shifan Qin, Haojie Jin, J.C. Koen van der Mijn, Arnout Schepers, Subramanian Venkatesan, Wenxin Qin, Roderick L. Beijersbergen, Liqin Wang, and René Bernards

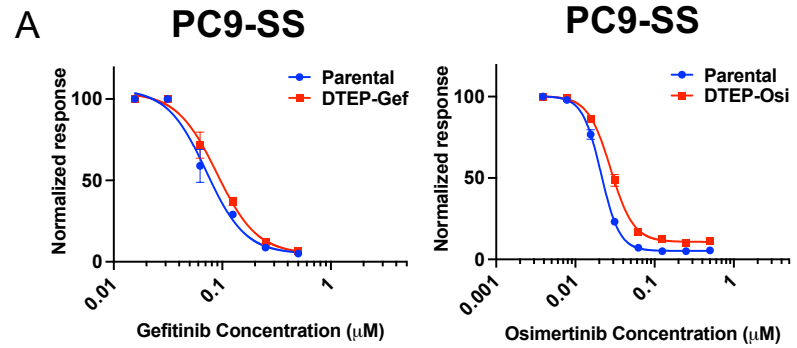

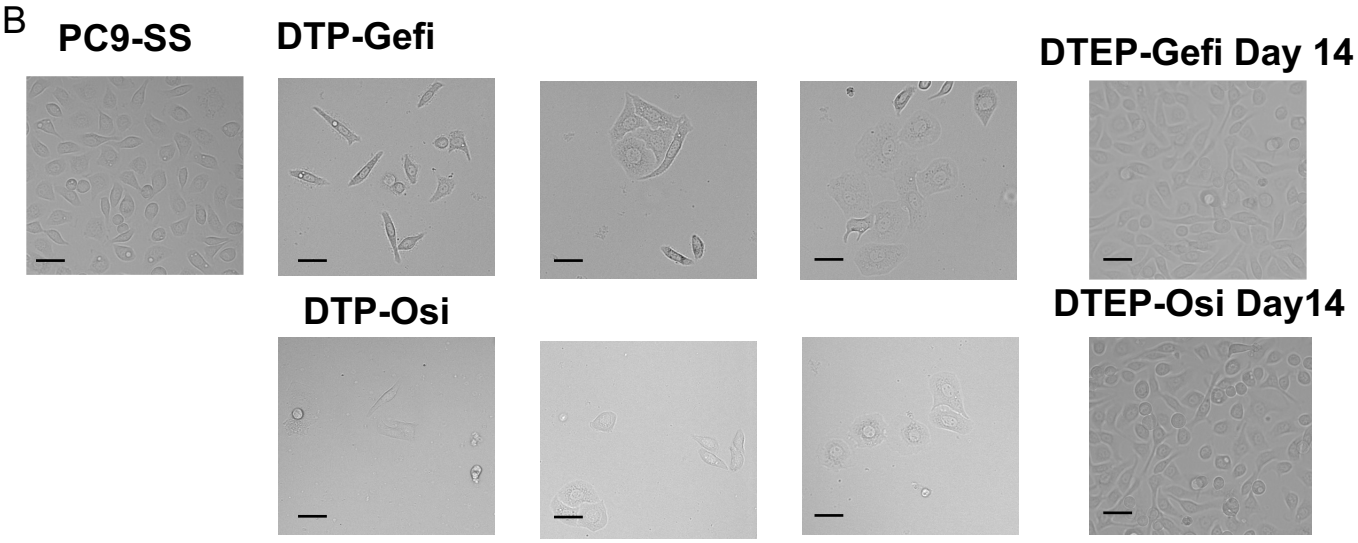

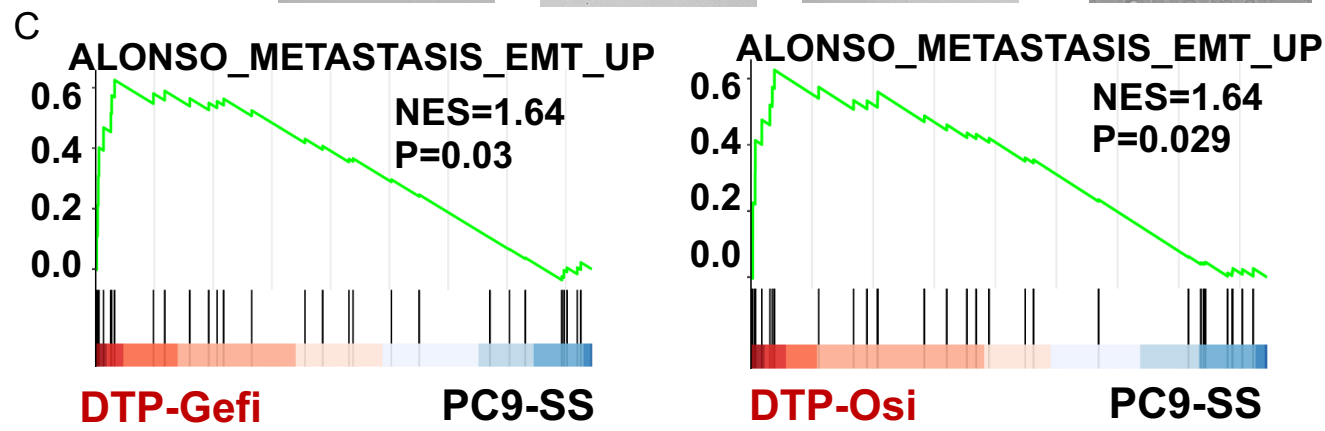

D

IC50	PC9-SS Gefitinib	PC9-SS Osimertinib	GTL-16 Crizotinib	A375 Dabra+Trame	H358 AMG510
Parental	71.23nM	21.08nM	117.4nM	11.49nM	16.42nM
DTEP	89.18nM	27.90nM	193.3nM	12.227nM	16.42nM

Figure S1. Persisters induction and purificaition in PC9, A375, GTL16 and H358. Related to Figures 1 and 2. (A) Five-day dose-response curve of DTPs and DTEPs to corresponding EGFR inhibitors. Error bars represent mean ± s.d., n = 3 independent experiments. Statistical significance was calculated by two-tailed Student's t-test. (B) Representative images of morphologies for Parental, DTP and DTEPs in PC9. Black scale bars, 50 μm. (C) GSEA analysis for EMT signature enrichment in DTPs in comparison with parental PC9 cells. (D) IC50 values to standard of care therapy in paired parental and DTEPs derived from PC9, GTL-16, A375 and H358. Days for culturing after drug wash out were 21, 30 and 14 for DTEPs derived from GTL-16, A375 and H358 accordingly. IC50, half-maximum inhibitory concentration.

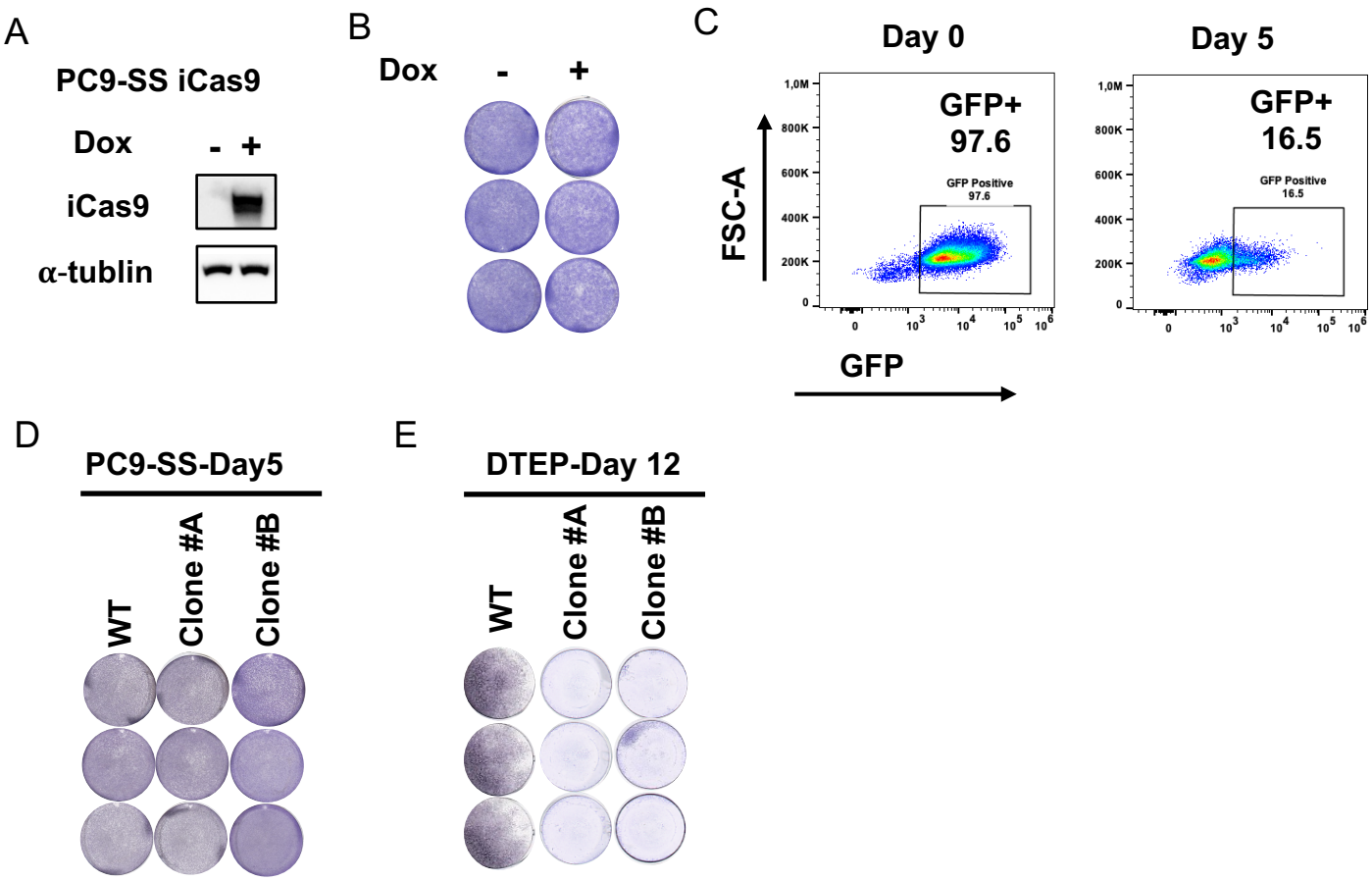

Figure S2. BRD2 knockout abolished the outgrowth of DTPs into DTEPs while had miner effect on proliferation of parental PC9 cells. Related to Figure 1.(A) Western blot detection of Cas9 expression after 24h Dox(doxycycline) treatment (1μg ml^{-1}). (B) Colony formation assay for PC9-SS iCas9 cells after 5 days Dox treatment (1μg ml^{-1}). Replicates were performed for each group. (C) Editing efficiency detection reflected by percentage of GFP positive cells after 10 days Dox treatment (1μg ml^{-1}). (D) Colony formation for WT and BRD2 knockout clones of PC9. Collected at day 5. (E) Long-term colony formation for WT and BRD2 knockout DTEPs induced by Osimertinib. Collected at day 12. Replicates were performed for each group.

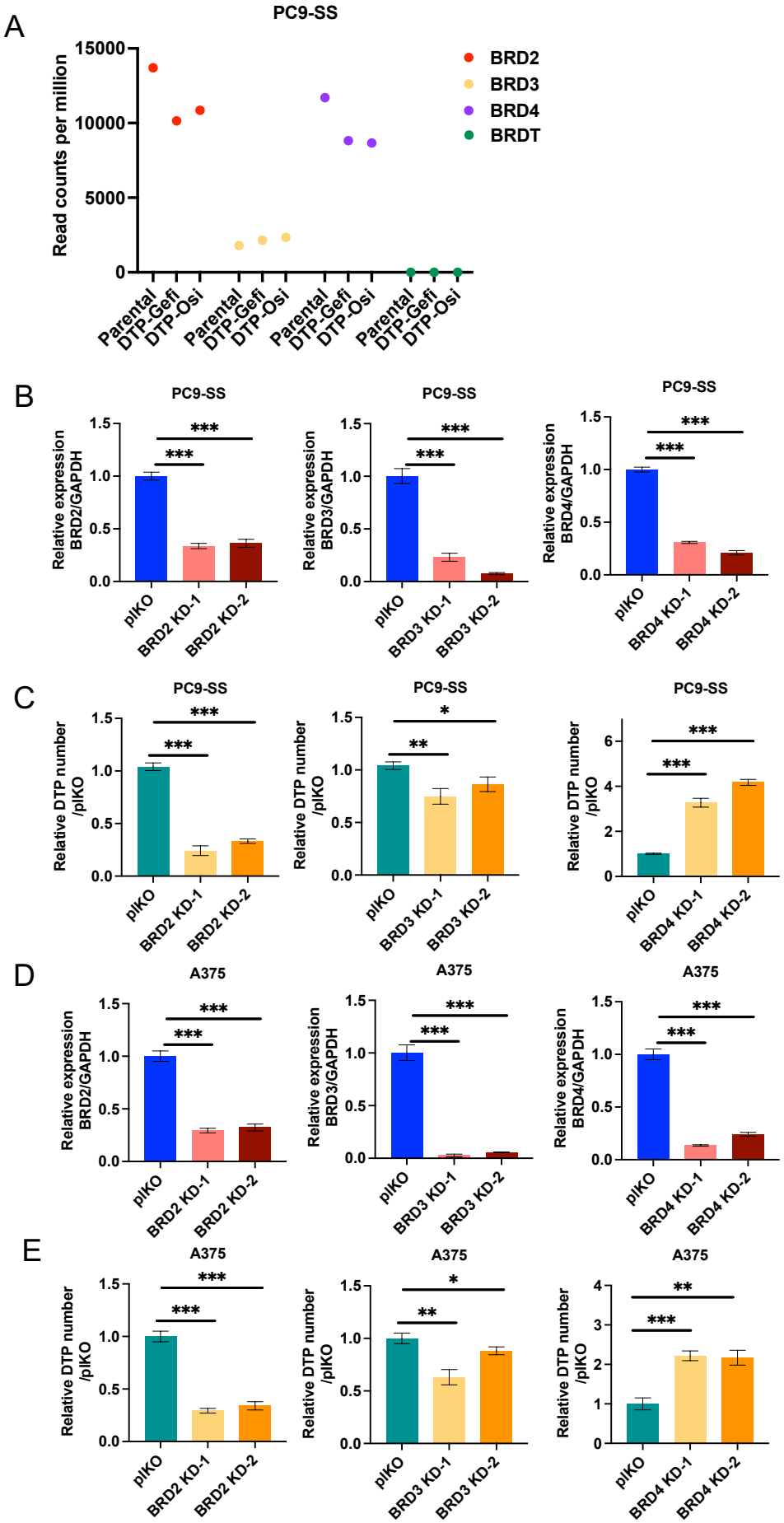

Supplementary Figure 3. DTP formation analysis in BRD2-4 knockdown cells in PC9 and A375. Related to Figures 1 and 2. (A) Read counts per million for BRD2-4 and BRDT in parental PC9, DTP-Gefi and DTP-Osi. (B) Knockdown efficiency of BRD2-4 by qRT-PCR in PC9. (C) DTP formation analysis in BRD2-4 knockdown groups as compared to plKO in PC9. (D) Knockdown efficiency of BRD2-4 by qRT-PCR in A375. (E) DTP formation analysis in BRD2-4 knockdown groups as compared to plKO in A375. Error bars in B-E represent mean ± s.d., n = 3 independent experiments. Statistical significance was calculated by two-tailed Student's t-test (*$P \leq 0.05$, ** $P \leq 0.01$, *** $P \leq 0.001$).

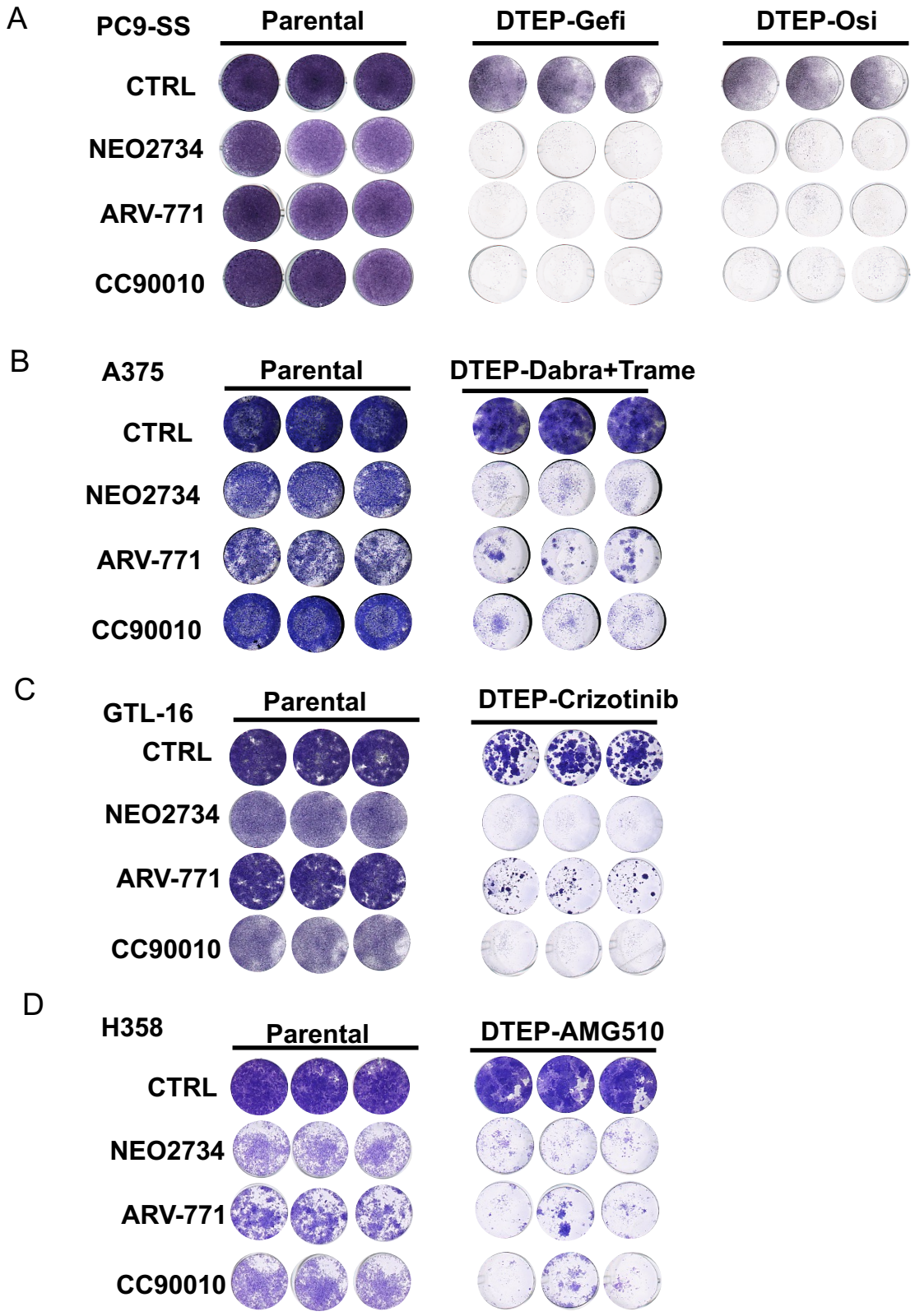

Figure S4. BET inhibitors suppress DTEPs validated by long-term colony formation assay. Related to Figures 1 and 2. (A-D) Long-term colony formation assay for paired parental and persisters from PC9, A375, GTL-16 and H358 treated with three BET inhibitors NEO2734, ARV-771 and CC90010. Parental were collected at Day 5. DTEPs were collected at day 12 except for GTL-16 collected at Day 21 (NEO2734: 0.08μM; ARV-771: 0.08μM; CC90010: 0.08μM). Replicates were performed for each group.

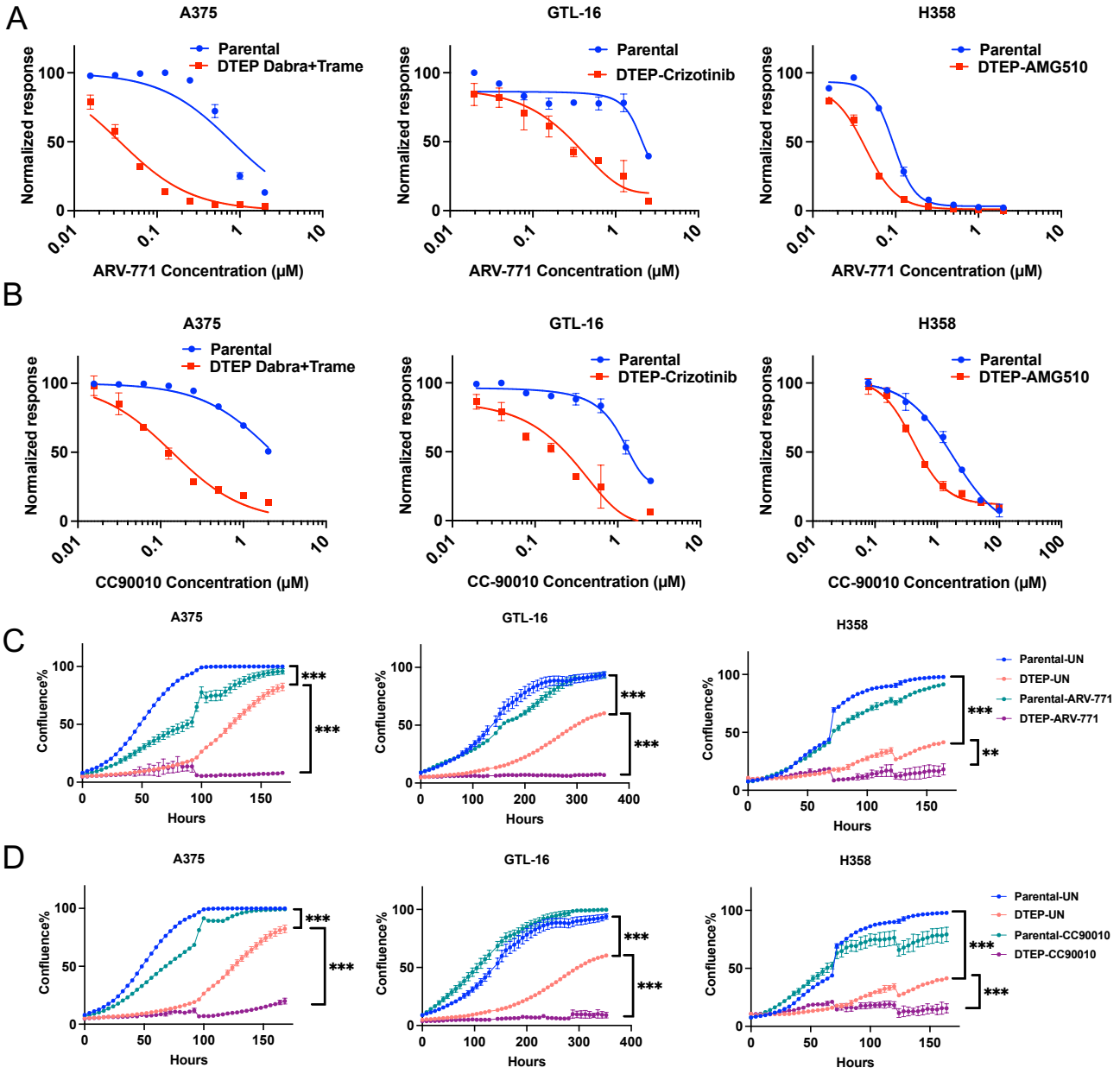

Figure S5. BET inhibitors suppress DTEPs validated by cell viability and incucyte growth monitoring. Related to Figure 2. (A) Five-day dose-response curve for paired parental and persisters from A375, GTL-16 and H358 to DMSO or BET inhibitor ARV-771. (B) Five-day dose-response curve for paired parental and persisters from A375, GTL-16 and H358 to DMSO or BET inhibitor CC90010. (C) Incucyte proliferation for paired parental and persisters from A375, GTL-16 and H358 treated with DMSO or ARV-771 (NEO2734: 0.08μM; ARV-771: 0.08μM; CC90010: 0.08μM). (D) Incucyte proliferation for paired parental and persisters from A375, GTL-16 and H358 treated with DMSO or CC90010 (NEO2734: 0.08μM; ARV-771: 0.08μM; CC90010: 0.08μM). Error bars in A-D represent mean ± s.d., n = 3 independent experiments. Statistical significance was calculated by two-tailed Student's t-test (*P ≤ 0.05, ** P ≤ 0.01, *** P ≤ 0.001).

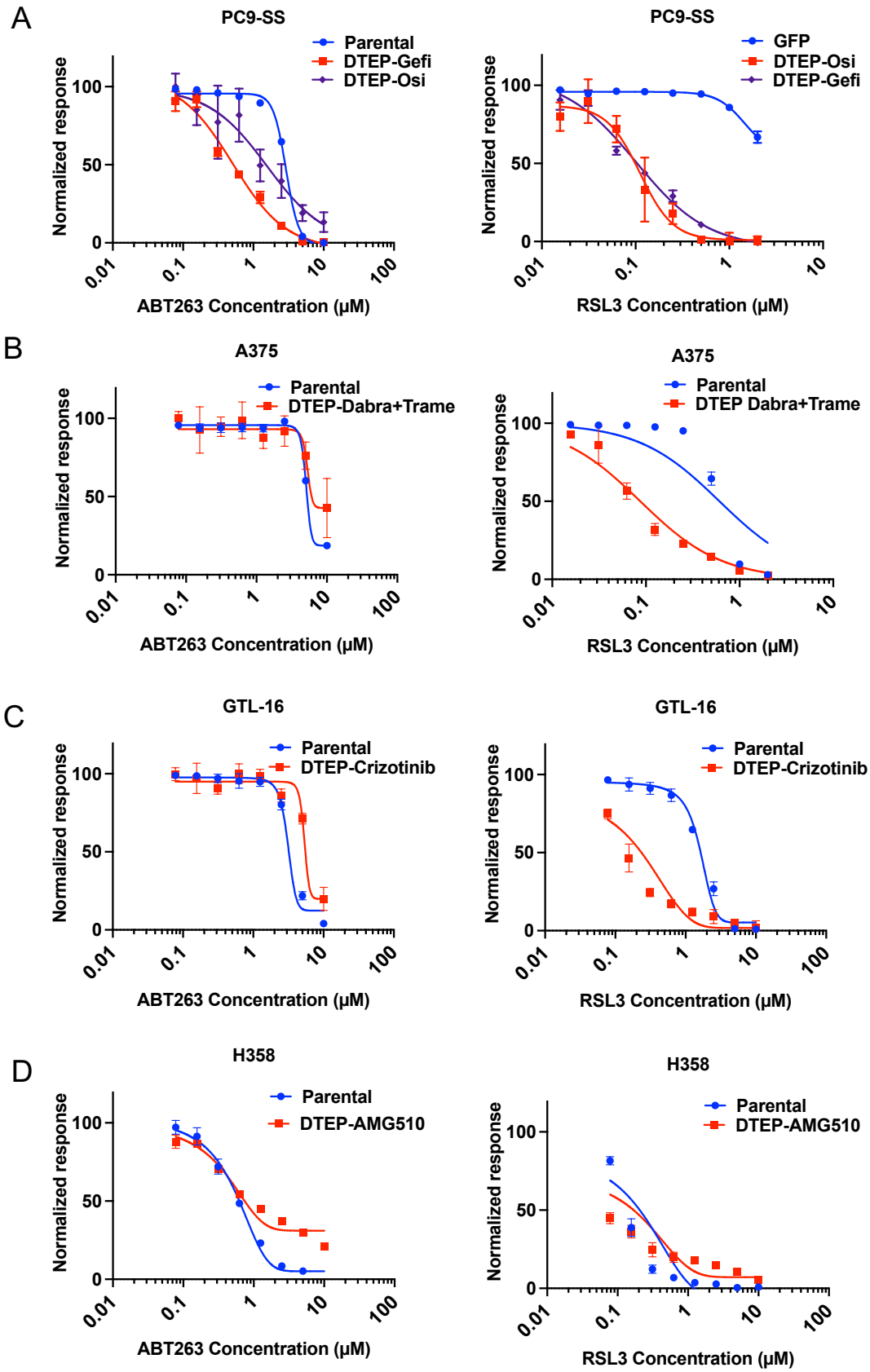

Figure S6. ABT263 selectively eliminated persisters derived from EGFPi induced PC9. No therapeutic window was observed from H358 treated with RSL3. Related to Figures 1 and 2. (A-D) Five-day dose response curve for paired parental and persisters from PC9, A375, GTL-16 and H358 to Bcl family inhibitor ABT263 and GPX4 inhibitor RSL3. Error bars in A-D represent mean ± s.d., n = 3 independent experiments. Statistical significance was calculated by two-tailed Student's t-test.

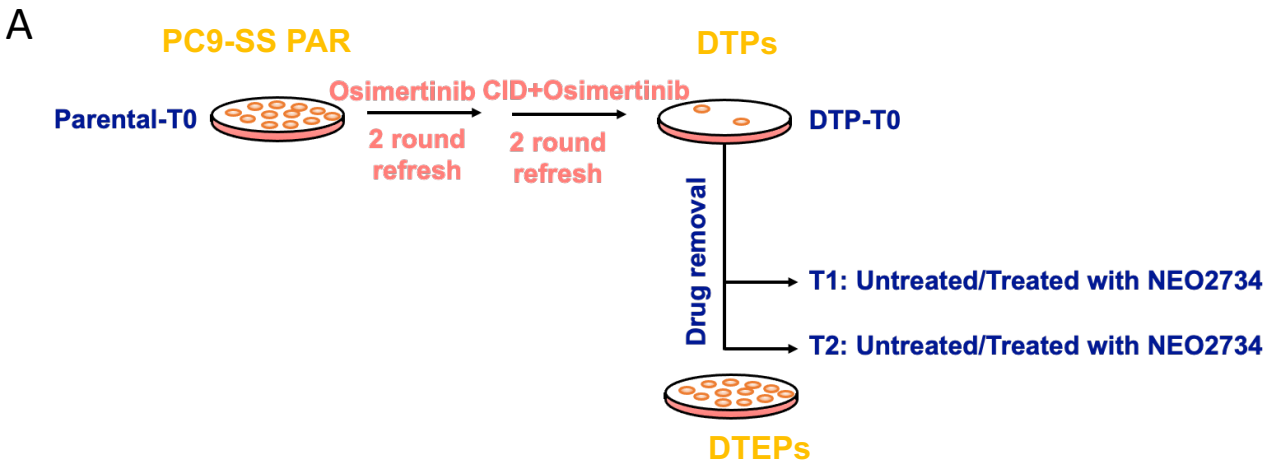

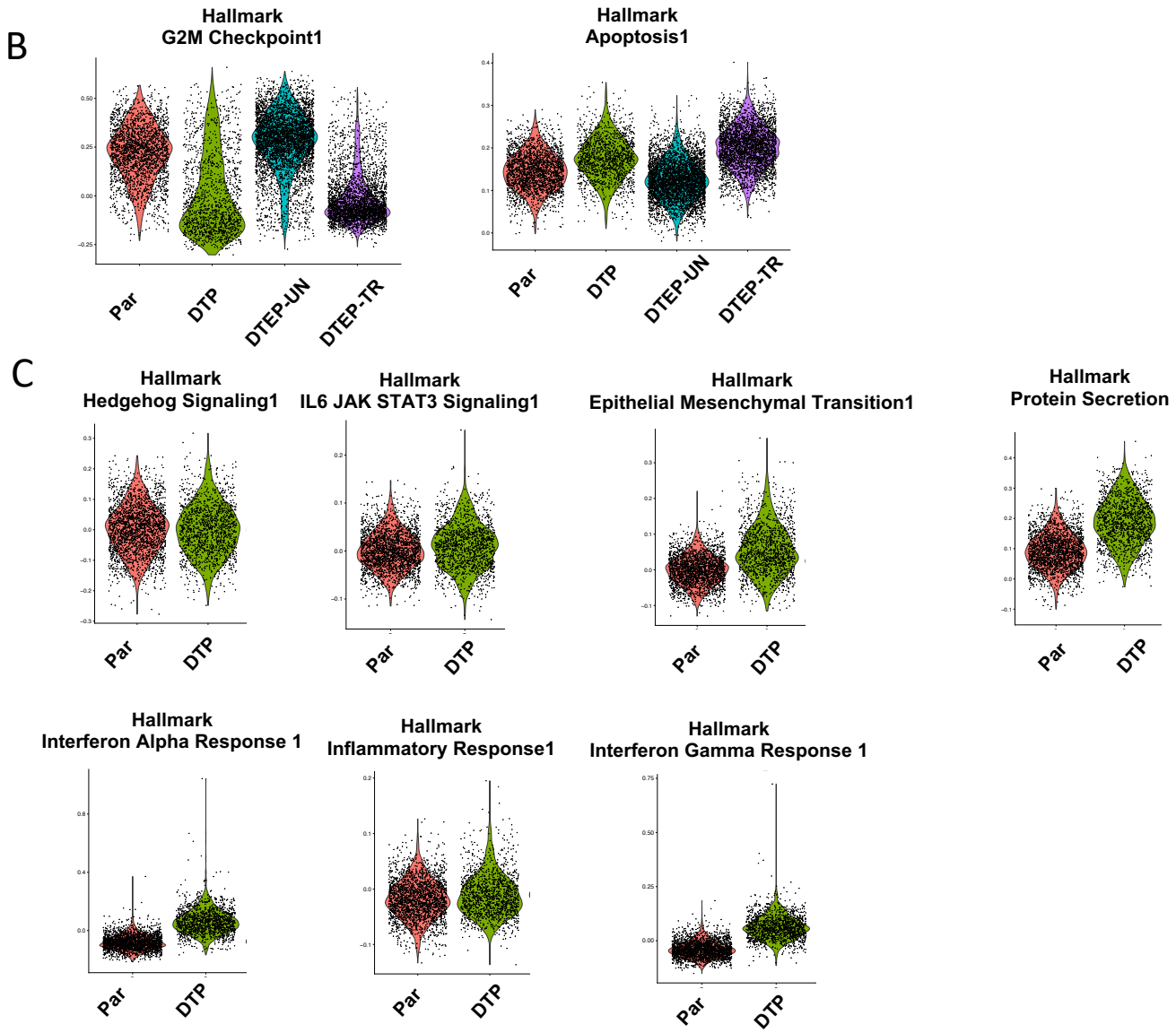

Figure S7. scRNA seq uncovered different gene signature in persisters. Related to Figure 3. (A) Graphic description of scRNA seq sample preparations. (B) Dynamic changes for G2M checkpoint and apoptosis observed in parental, DTP, DTEP and DTEP treated with NEO2734. (C) Representative gene signatures identified in DTPs.

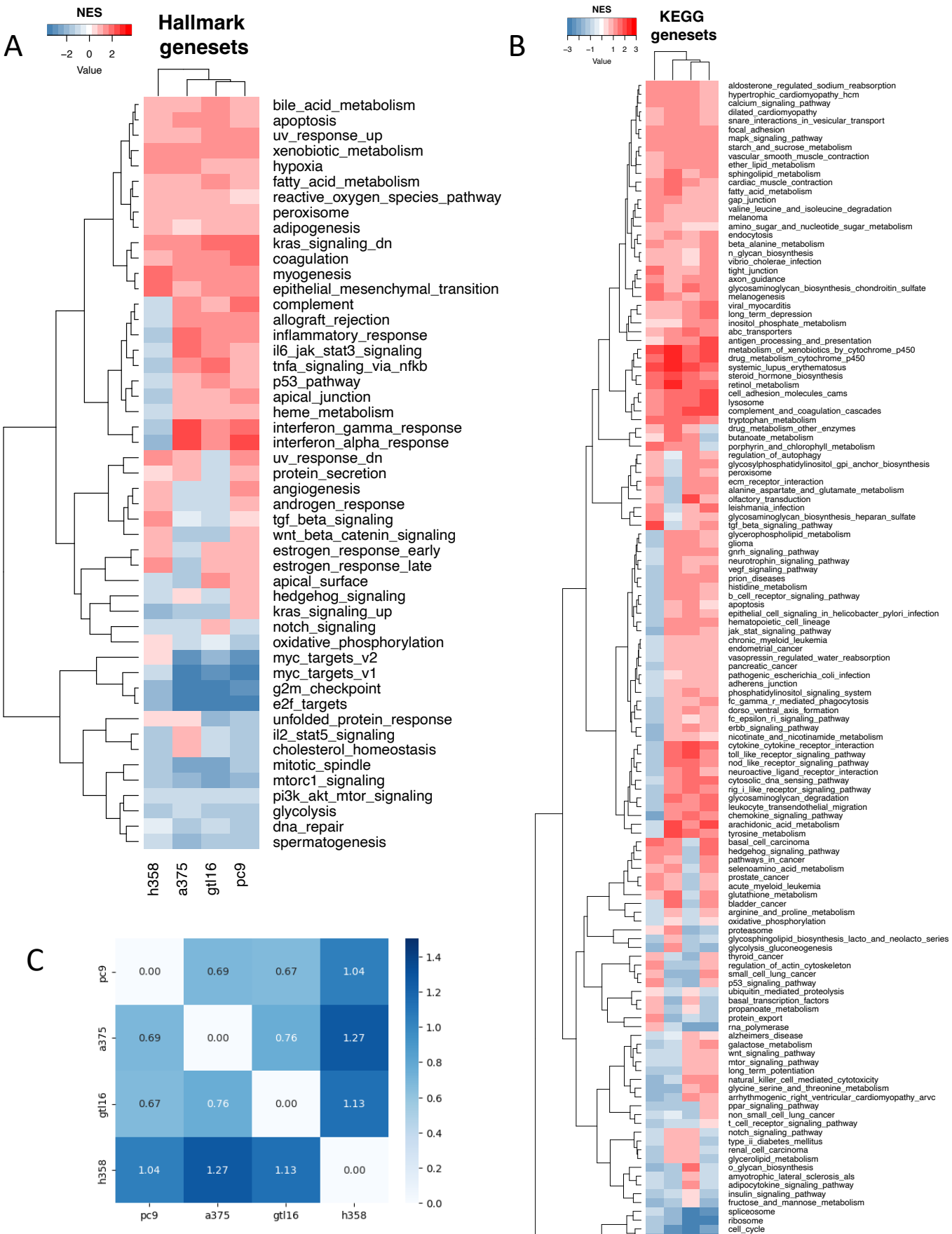

Figure S8. bluk RNA seq based transcriptomic features of DTPs compared with parental controls. Related to Figure 3. (A) GSEA pathway enrichment analysis for DTPs compared with parental controls focusing on Hallmark genesets. (B) GSEA pathway enrichment analysis for DTPs compared with parental controls focusing on KEGG genesets. (C) Heatmap representation for distance among each NES score for paried DTP T0/Parental T0 based on GSEA analysis for both Hallmark and KEGG genesets.

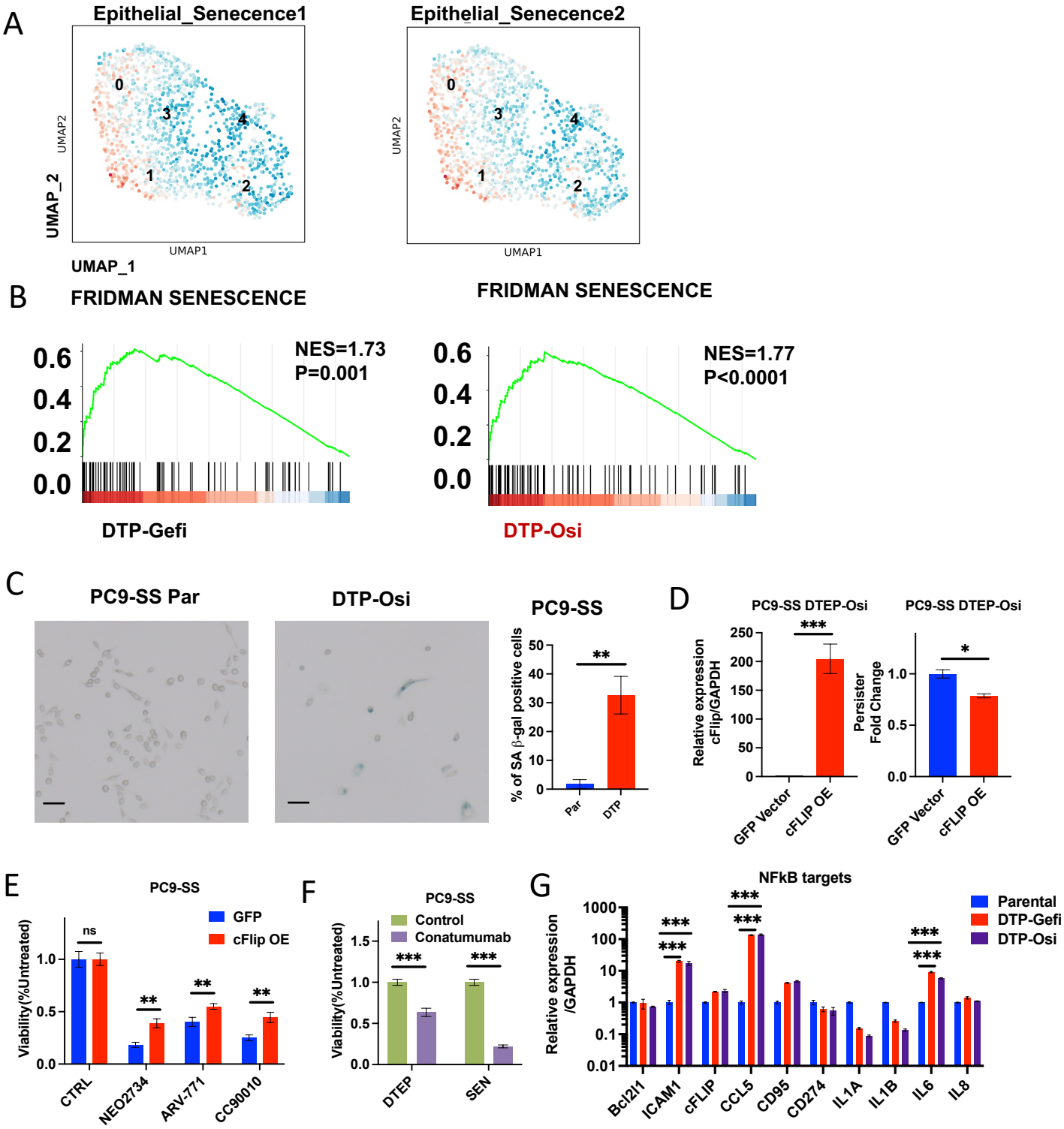

Figure S9. DTPs share some similarities with senescence cells but have different vulnerabilities. Related to Figure 3.
(A) Senesence signature geneset modula score within DTPs. Two epithelial senescence signatures were tested. (B) GSEA analysis for senescence gene signature in DTPs in comparison with parental PC9 cells based on bulk-RNA seq. (C) Senescence-associated β-galactosidase (SA-β-Gal) staining of cells. Left: Representative image; Right: Quantification of left. Black scale bars, 50 µm. (D) cFLIP overexpression efficiency detected by qPCR. Persister cells calculation compared to GFP control. (E) Relative viabilities of DTEPs from GFP and cFLIP^{OE} PC9 treated with three BET inhibitors. NEO2734: 0.08µM; ARV-771: 0.08µM; CC90010: 0.08µM. (F) Relative viabilities of DTEPs and senescent cells from GFP and cFlip^{OE} PC9 treated with Conatumumab. Conatumumab:125ng/ml. (G) Transcriptomic analysis of NF-kB targets in parental PC9, DTP-Gefi and DTP-Osi. Error bars in C-G represent mean ± s.d., n = 3 independent experiments. Statistical significance was calculated by two-tailed Student's t-test (*P ≤ 0.05, ** P ≤ 0.01, *** P ≤ 0.001).

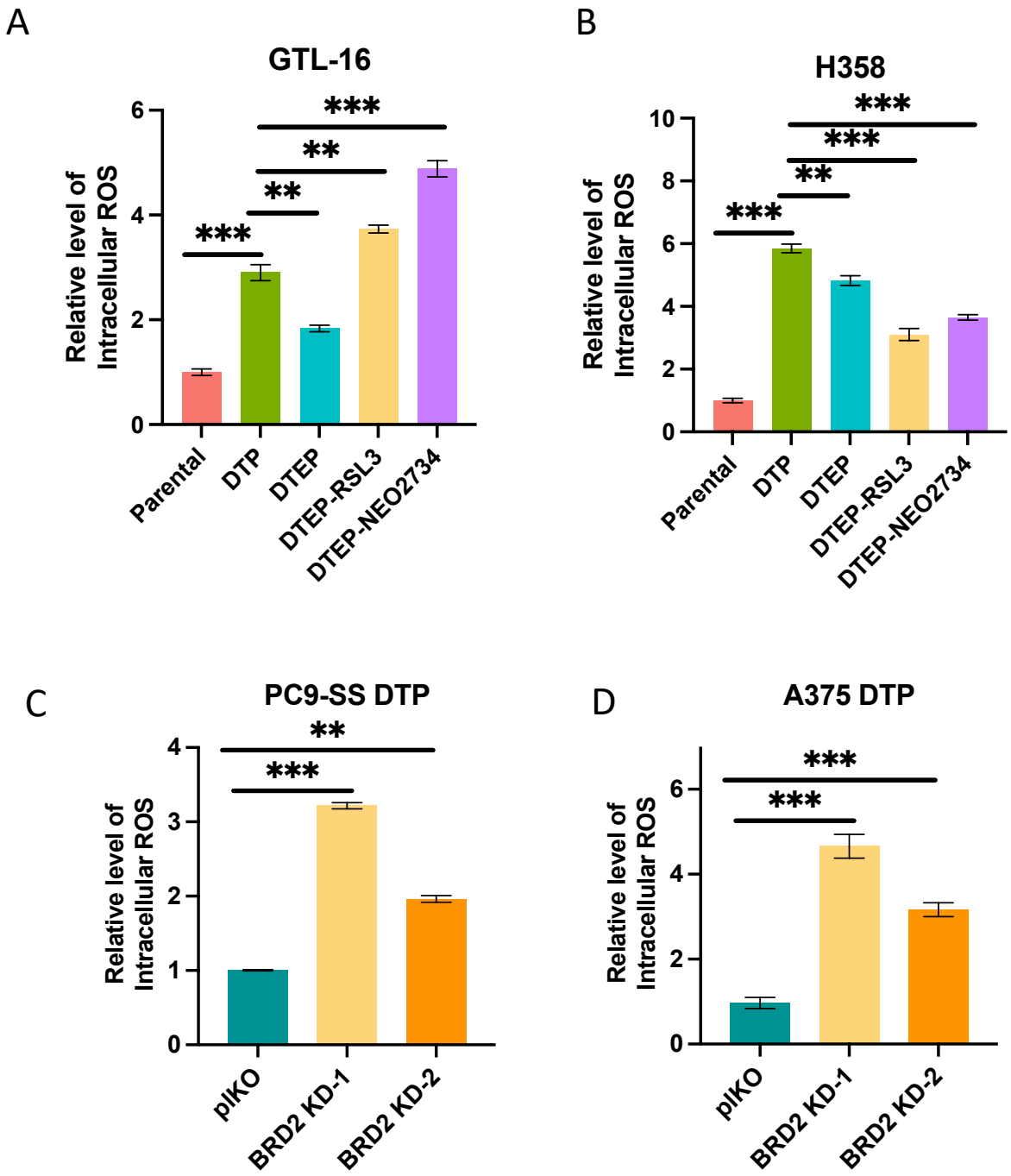

Figure S10. Intracellular ROS staining by flow cytometry in GTL-16 and H358. Related to Figures 4 and 5. (A) Quantifications of intracellular ROS level (mean fluorescent intensity) in parental GTL-16, DTP, DTEP and DTEP challenged with RSL3 and NEO2734. (B) Quantifications of intracellular ROS level (mean fluorescent intensity) in parental H358, DTP, DTEP and DTEP challenged with RSL3 and NEO2734. (C) Quantifications of intracellular ROS level (mean fluorescent intensity) of DTPs from BRD2 knockdown cells compared to plKO cells in PC9-SS. (D) Quantifications of intracellular ROS level (mean fluorescent intensity) of DTPs from BRD2 knockdown cells compared to plKO cells in PC9-SS. Error bars in A-D represent mean ± s.d., n = 3 independent experiments. Statistical significance was calculated by two-tailed Student's t-test (*P ≤ 0.05, ** P ≤ 0.01, *** P ≤ 0.001).

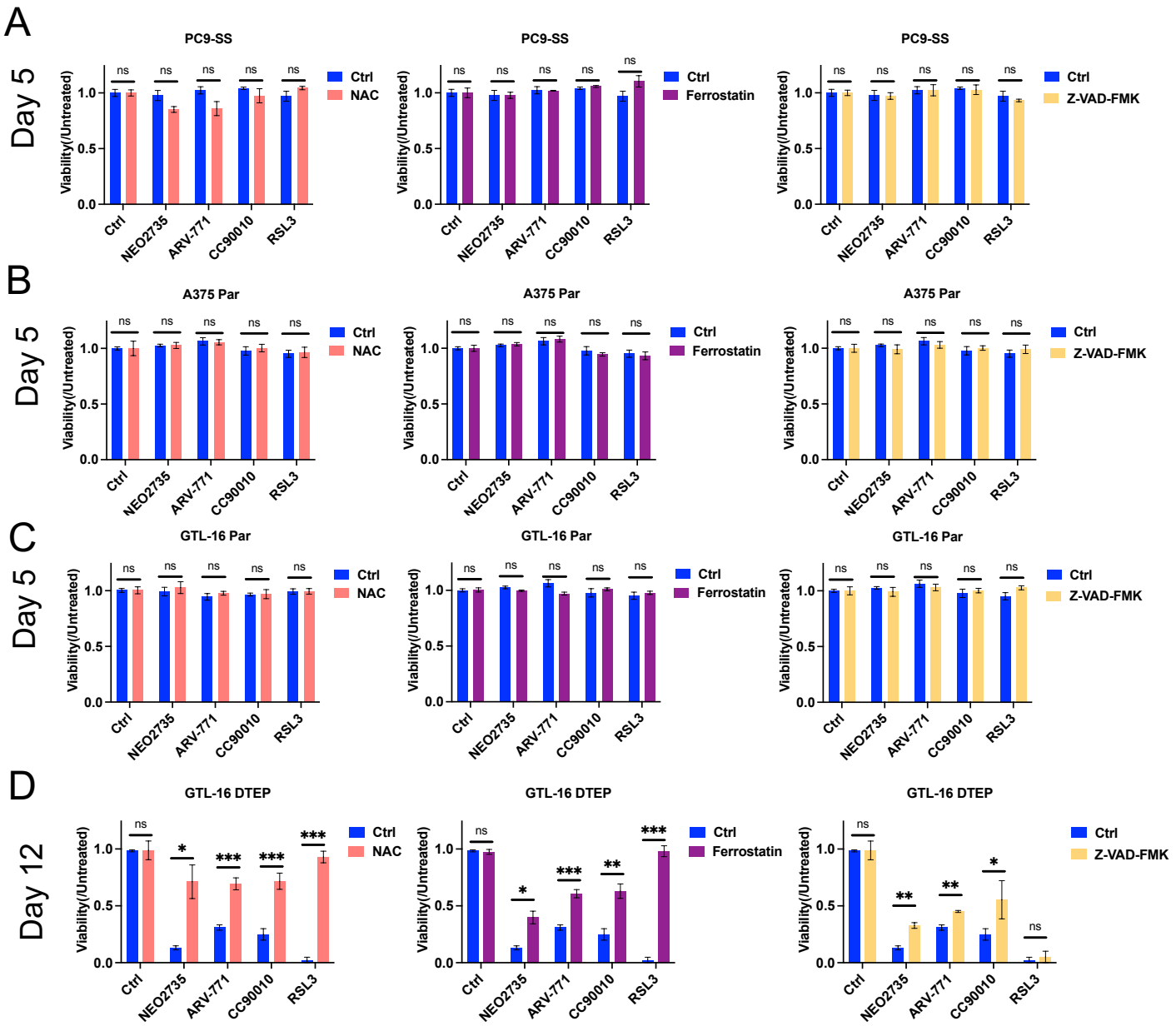

Figure S11. Rescue experiments by NAC, Ferrostatin and Z-VAD-FMK in PC9, A375 and GTL-16 derived DTEPs treated with BET inhibitors. Related to Figures 4 and 5. (A) Relative cell viabilities of parental PC9 treated with NEO2734, ARV-771, CC90010 and RSL3 cultured with or without NAC, Ferrostatin and Z-VAD-FMK. (B) Relative cell viabilities of parental A375 treated with NEO2734, ARV-771, CC90010 and RSL3 cultured with or without NAC, Ferrostatin and Z-VAD-FMK. (C) Relative cell viabilities of parental GTL-16 treated with NEO2734, ARV-771, CC90010 and RSL3 cultured with or without NAC, Ferrostatin and Z-VAD-FMK. (D) Relative cell viabilities of DTEP derived from GTL-16 treated with NEO2734, ARV-771, CC90010 and RSL3 cultured with or without NAC, Ferrostatin and Z-VAD-FMK (NEO2734: 0.25μM; ARV-771: 0.25μM; CC90010: 0.25μM; NAC:2.5mM; Ferrostatin: 2.5μM; Z-VAD-FMK: 10μM). Error bars in A-D represent mean ± s.d., n = 3 independent experiments. Statistical significance was calculated by two-tailed Student's t-test (*P ≤ 0.05, ** P ≤ 0.01, *** P ≤ 0.001).

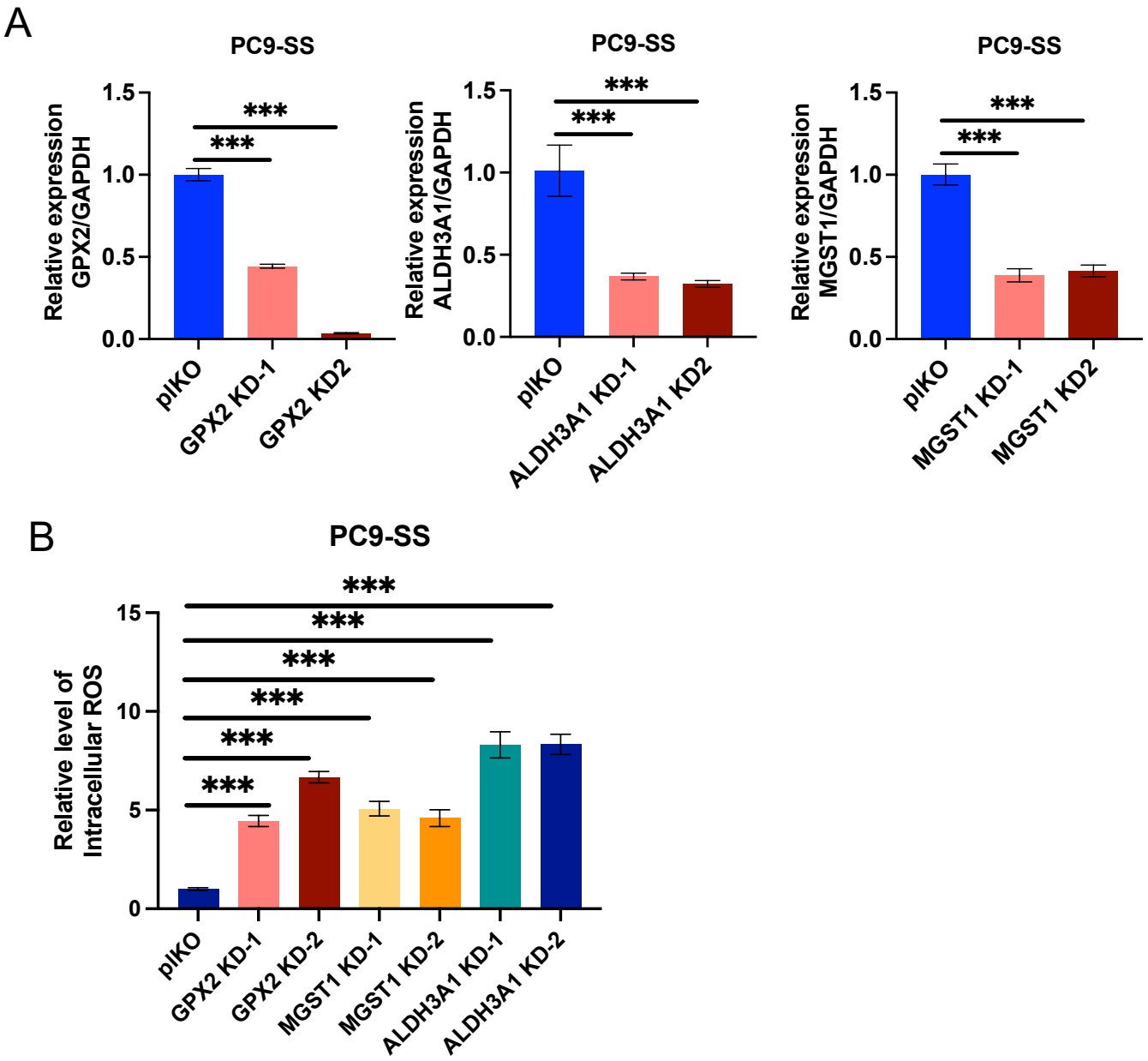

Figure S12. ROS level of DTPs were increased upon knockdown of GPX2, ALDH3A1 and MGST1. Related to Figure 5. (A) Knockdown efficiency of GPX2, MGST1 and ALDH3A1 in PC9-SS by q-PCR. (B) Quantification of intracellular ROS levels (mean fluorescent intensity) of DTPs in plKO, GPX2 KD-1, GPX2-KD2, MGST 1 KD-1, MGST1 KD-2, ALDH3A1 KD-1 and ALDH3A1 KD-2. Error bars in A-B represent mean ± s.d., n = 3 independent experiments. Statistical significance was calculated by two-tailed Student's t-test (*$P \leq 0.05$, ** $P \leq 0.01$, *** $P \leq 0.001$).

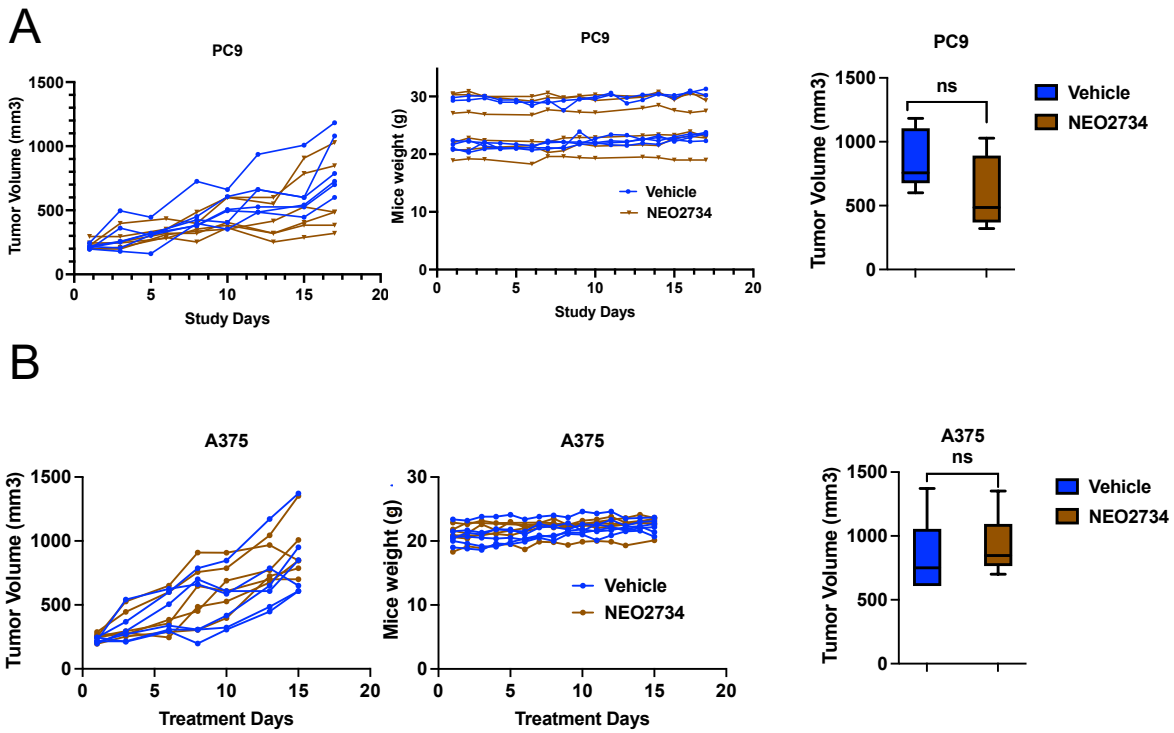

Figure S13. BET inhibitor has minor effect on controlling parental cancer proliferation in vivo. Related to Figure 6. (A) Relative tumor volumes and mice weight for PC9 subcutaneous bearing mice treated with vehicle, NEO2734 (n=6 for each group). (B) Relative tumor volumes and mice weight for A375 subcutaneous bearing mice treated with vehicle, NEO2734 (n=6 for each group). Data are presented as mean ± s.e.m. Two-way analysis of variance (ANOVA) was applied for the in vivo study statistical analysis (*$P \leq 0.05$, ** $P \leq 0.01$, *** $P \leq 0.001$).

Table S2. List of DTP markers and their expression changes in DTEPs upon NEO2734 treatment. Related to Figure 3.

DTP markers	Log2 FC(DTEP TR/UN)	Aver_Differ
ALDH3A1	-4,24792751	1,89131446
CYP1B1	-3,86882918	10,2313782
LYPD6B	-2,37178861	23,6253318
GPX2	-2,15881489	11,0704595
FN1	-1,88328188	5,21058898
ALPP	-1,7684921	8,15688063
S100P	-1,75822321	4,73060596
CCDC80	-1,58230944	6,14430032
SERPINB5	-1,495077	4,03732768
VGLL1	-1,47196457	5,11506143
MGST1	-1,3721061	2,78435996
FXYD3	-1,32192809	16,7187148
IGFBP3	-1,32125574	6,83528438
FBP1	-1,30142978	12,4883401
ARHGDIB	-1,17023692	11,0335559
RBM47	-1,12890212	24,5836547
TPD52L1	-1,12657188	5,84317502
CXXC5	-0,94981424	7,57707816
TNS3	-0,91737317	18,3930842
RPL37	-0,87334095	0,74569086
CAMK2N1	-0,78580473	17,7801061
GNAQ	-0,78300339	12,346179
PCDH7	-0,77356121	7,18389647
PLS3	-0,71814063	7,81059494
TNFAIP2	-0,68492254	8,1285217
MAL	-0,67855938	18,0648175
PRXL2A	-0,67719781	4,61986633
TMEM45B	-0,60847331	6,9806803
MARCKS	-0,57872439	9,97916452
LIMCH1	-0,53476096	11,1598565
CDKN2A	-0,49811924	15,1279592
LCN2	-0,48433738	2,93410644
CAMK2G	-0,46497628	16,2216722
CTSD	-0,4358519	0,19504952
CTSH	-0,38861432	5,82573071
RPS12	-0,38145905	0,36583016
SKIL	-0,35361539	10,7074503
TMEM139	-0,2833068	13,8833255
ATXN10	-0,27397375	6,04671629
PLAAT3	-0,22948185	10,6750645
MUC20	-0,15600502	6,74053935

DAPK1	-0,10568917	14,3203738
PSCA	-0,03783207	6,56881003
PDLIM1	0,09297777	17,0282715
SH3YL1	0,13521414	10,1606966
EZR	0,18473501	4,89626196
FBLN1	0,22287053	8,47485305
ANXA4	0,23157893	8,29378063
PDGFD	0,24259765	11,3406825
TSTD1	0,24392558	12,0886066
MT-CO3	0,25691449	6,64883653
PCSK5	0,47978787	5,54494723
SEMA5A	0,48122412	9,11149452
GSTK1	0,5687882	21,7718524
JDP2	0,56889181	14,031336
SPINT2	0,57939187	1,48930862
CD9	0,62002364	4,84567969
MAN1A1	0,74029976	18,6314181
QPRT	0,80279664	15,2491275
ASAH1	0,85656868	9,81037049
KRT7	0,86098473	2,181738
LGALS3	0,98274867	20,0718399
KRT19	1,12169516	1,4909795
GABARAP	1,14438991	4,29122683
MYH14	1,16021737	24,5180585
TRAPPC6A	1,17632277	8,29220981
CD24	1,24603979	15,6185246
TACSTD2	1,258863	3,34741067
TMC4	1,43609911	7,5342684

Table S3. List of primers. Related to Figures 1&5 and STAR Methods.

qPCR primers

Name	**Sequence**
ALDH3A1-F	TGGAACGCCTACTATGAGGAG
ALDH3A1-R	GGGCTTGAGGACCACTGAG
MGST1-F	GCCCACCTGAATGACCTTGA
MGST1-R	GTCTGAAGTGCAGGATGGCT
GPX2-F	GACTTCACCCAGCTCAACGA
GPX2-R	CCCCAGGACGGACATACTTG
GAPDH-F	GAAGGTGAAGGTCGGAGTC
GAPDH-R	GAAGATGGTGATGGGATTTC
cFlip-F	GTTCAAGGAGCAGGGACAAG
cFlip-R	TCCCATTTATGGAGCCTGAAG
BCL2L1-F	GTAAACTGGGGTCGCATTGT
BCL2L1-R	TGGATCCAAGGCTCTAGGTG
ICAM1-F	ATGCCCAGACATCTGTGTCC
ICAM1-R	GGGGTCTCTATGCCCAACAA
CCL5-F	CCAGCAGTCGTCTTTGTCAC
CCL5-R	CTCTGGGTTGGCACACACTT
CD95-F	TCTGGTTCTTACGTCTGTTGC
CD95-R	CTGTGCAGTCCCTAGCTTTCC
CD274-F	TATGGTGGTGCCGACTACAA
CD274-R	TGGCTCCCAGAATTACCAAG
IL-1A-F	AGATGCCTGAGATACCCAAAACC
IL-1A-R	CCAAGCACACCCAGTAGTCT
IL-1B-F	AAGCCCTTGCTGTAGTGGTG
IL-1B-R	GAAGCTGATGGCCCTAAACA
IL-6-F	ACTCACCTCTTCAGAACGAATTG
IL-6-R	CCATCTTTGGAAGGTTCAGGTTG
IL-8-F	TCCTGATTTCTGCAGCTCTGT
IL-8-R	AAATTTGGGGTGGAAAGGTT
BRD2-F	GAGGTGTCCAATCCCAAAAAGC
BRD2-R	ATGCGAACTGATGTTTCCACA
BRD3-F	CTGAAACCCACCACTTTGCG
BRD3-R	GCTCCTCTTTCGACTTGGCT
BRD4-F	ACCTCCAACCCTAACAAGCC
BRD4-R	TTTCCATAGTGTCTTGAGCACC

shRNA sequence:

shBRD2#1	CCGGGCCCTCTTTACGTGATTCAAACTCGAGTTTGAATCACGTAAAGAGGGCTTTTT
shBRD2#1	CCGGCCCTGCCTACAGGTTATGATTCTCGAGAATCATAACCTGTAGGCAGGGTTTTT
shBRD3#1	CCGGCCCAAGAGGAAGTTGAATTATCTCGAGATAATTCAACTTCCTCTTGGGTTTTT
shBRD3#2	CCGGGCTGATGTTCTCGAATTGCTACTCGAGTAGCAATTCGAGAACATCAGCTTTTT
shBRD4#1	CCGGCCTGGAGATGACATAGTCTTACTCGAGTAAGACTATGTCATCTCCAGGTTTTTG
shBRD4#2	CCGGCCCTTTGCTGTGACACTTCTTCTCGAGAAGAAGTGTCACAGCAAAGGGTTTTT
shGPX2#1	CCGGCCTTGCAACCAATTTGGACATCTCGAGATGTCCAAATTGGTTGCAAGGTTTTTG
shGPX2#2	CCGGCCGATCCCAAGCTCATCATTTCTCGAGAAATGATGAGCTTGGGATCGGTTTTTG
shALDH3A1#1	CCGGGCTAAGAAATCCCGGGACTATCTCGAGATAGTCCCGGGATTTCTTAGCTTTTT
shALDH3A1#2	CCGGCCTGCACAAGAATGAATGGAACTCGAGTTCCATTCATTCTTGTGCAGGTTTTT
shMGST1#1	CCGGGCCAATATCCTGTATTCTTGTCTCGAGACAAGAATACAGGATATTGGCTTTTTTG
shMGST1#2	CCGGCATACAACTCAGCATCCAGTTCTCGAGAACTGGATGCTGAGTTGTATGTTTTTG